ISBN: 978-3-95450-200-4 doi:10.18429/JACoW-ICAP2018-MOPAF04

SPIN DYNAMICS IN MODERN ELECTRON STORAGE RINGS: COMPUTATIONAL ASPECTS

Oleksii Beznosov*, James A. Ellison, Klaus A. Heinemann, UNM, Albuquerque, NM, USA
Desmond P. Barber[1], DESY, Hamburg, Germany
Daniel Appelö, University of Colorado, Boulder, CO, USA
[1] also at UNM, Albuquerque, NM, USA

INTRODUCTION

In [1] we report on our spin/polarization project for understanding the possibility of polarization for the next generation of the high energy particle (HEP) accelerators, e.g., the Future Circular Collider (FCC) and Circular Electron Positron Collider (CEPC). The physics background and the basic model to compute the polarization is discussed there. The starting point is what we call the full Bloch equation (FBE) in the Lab frame. This model includes synchrotron radiation and the concomitant depolarization from the radiation caused by damping and diffusion as well as Sokolov-Ternov spin-flip polarization effects and its Baier-Katkov generalization. Ignoring spin flip we obtain the reduced Bloch equation (RBE) which we believe contains the most difficult part of the FBE to integrate numerically. We then introduce the 3 degree of freedom (DOF) reduced Bloch equation (RBE) in the beam frame in the first section below. We further discuss the general computational issues and give an estimates for what can be done with current computational techniques. For $d = \{1, 2, 3\}$ DOF the polarization density has $(2d + 1)$ independent variables. For simplicity, suppose that each of the space-like variables has been discretized on a grid with N grid-points, then the computational cost of each time step will scale no better than $O(N^{2d})$. The presence of parabolic terms in the governing equations necessitates implicit time stepping and thus solutions of linear systems of equations. For a fully coupled 3 DOF problem this will bring the per time step cost to $O(N^{6q})$, with $1 \leq q \leq 3$, depending on the algorithms used for the linear solve. However, only algorithms with $q \approx 1$ are feasible (for Gaussian elimination $q = 3$). Fortunately, as we outline below, the structure of the averaged equations (e.g the parabolic terms are uncoupled from mode coupling terms) allows the efficient parallel implementation. Further, we exploit the decoupling by evolving the resulting ODE system with the additive Runge-Kutta (ARK) method. Described in [2] ARK methods are high order semi-implicit methods that are constructed from a set of consistent Runge-Kutta (RK) methods. In the RBE the parabolic part of the equation is treated with a diagonally implicit RK method (DIRK) and the hyperbolic mode coupling part is treated with an explicit RK (ERK) method which does not require a linear solve. The ODE system in time can be evolved independently for each Fourier mode resulting in a computational cost for each timestep that scales as $O(N^{3q})$ per mode.

We first summarize the 3 DOF problem and 2 DOF problem from [1]. Then we describe the new algorithm on the example of 1 DOF model with parameters taken from the Hadron-Electron Ring Accelerator (HERA). Using that the RBE in 1 DOF can be solved exactly we demonstrate the accuracy of the algorithm by compering the exact polarization to the polarization measured by integrating the numerical solution in space. Further, we present the results showing that achieved accuracy of the algorithm for the polarization density after 1500 turns for varying discretization parameters which allows us to conclude that the algorithm is feasible for the accurate simulation of the 3 DOF model.

* Corresponding author: obeznosov@unm.edu

RBE IN 3 DEGREES OF FREEDOM

Consider the system of Langevin equations for the orbital phase space variable $Y \in \mathbb{R}^6$ and the spin variable $\vec{S}$ in the beam frame given by

$$Y' = \mathcal{A}(\theta)Y + \sqrt{\varepsilon}\sqrt{\omega(\theta)}e_6\xi(\theta), \tag{1}$$

$$\vec{S}' = \Omega_Y(\theta, Y)\vec{S}. \tag{2}$$

Here θ is the accelerator azimuth and ξ is a version of the white noise process and $e_6 = (0, 0, 0, 0, 0, 1)^T$. Also $\mathcal{A}(\theta)$ is a 6×6 matrix encapsulating radiationless motion and the deterministic effects of synchrotron radiation (see, e.g., [3, eq. 5.3]). Moreover $\Omega_Y(\theta, Y)$ in the Thomas-BMT term is a skew-symmetric 3×3 matrix linear in Y and $\omega(\theta)$ is real valued. Note also that $\mathcal{A}(\theta)$, $\Omega_Y(\theta, y)$ and $\omega(\theta)$ are 2π-periodic in θ.

The RBE for the polarization density $\vec{\eta}_Y$ is

$$\partial_\theta \vec{\eta}_Y = (L_Y + L_{Y,TBMT})\vec{\eta}_Y, \tag{3}$$

where

$$L_Y = \overbrace{-\sum_{j=1}^{6} \partial_{y_j}\Big(\mathcal{A}(\theta)y\Big)_j}^{\text{Drift}} + \overbrace{\frac{1}{2}\omega_Y(\theta)\partial_{y_6}^2}^{\text{Diffusion}},$$

$$L_{Y,TBMT}\vec{\eta}_Y = \underbrace{\Omega_Y(\theta, y)\vec{\eta}_Y}_{\text{Spin}}.$$

Our ultimate aim is to understand the solutions of (3). The main quantity of interest is the polarization of the bunch

$$\vec{P}(\theta) = \int \vec{\eta}_Y(\theta, y)dy.$$

However, as noted in the introduction, numerical discretization of (3) will have the an enormous computational cost. To simplify the problem we first use the method of averaging.

ISBN: 978-3-95450-200-4 doi:10.18429/JACoW-ICAP2018-MOPAF04

We split $\mathcal{A} = A + \varepsilon\delta A$ to isolate the Hamiltonian part A. Then by using the fundamental solution matrix $X(\theta)$ of the unperturbed problem, e.g

$$X' = A(\theta)X, \tag{4}$$

the method averaging Y-frame transforms to a V-frame associated with averaged problem posed in terms of the new variable V. In the V-frame the polarization density η_V satisfies the RBE

$$\partial_\theta \vec{\eta}_V = (L_V + L_{V,TBMT})\vec{\eta}_V, \tag{5}$$

where

$$L_V = \overbrace{-\varepsilon \sum_{j=1}^{6} \partial_{\mathrm{v}_j}(\bar{\mathcal{D}}\mathrm{v})_j}^{\text{Drift}} + \overbrace{\frac{\varepsilon}{2}\sum_{i,j=1}^{6} \bar{\mathcal{E}}_{ij}\partial_{\mathrm{v}_i}\partial_{\mathrm{v}_j}}^{\text{Diffusion}}, \tag{6}$$

$$L_{V,TBMT}\vec{\eta}_V = \underbrace{\Omega_Y(\theta, X(\theta)\mathrm{v})\vec{\eta}_V}_{\text{Spin}}. \tag{7}$$

and

$$\bar{\mathcal{D}} = \begin{pmatrix} \mathcal{D}_I & 0_{2\times2} & 0_{2\times2} \\ 0_{2\times2} & \mathcal{D}_{II} & 0_{2\times2} \\ 0_{2\times2} & 0_{2\times2} & \mathcal{D}_{III} \end{pmatrix}, \tag{8}$$

$$\mathcal{D}_\alpha = \begin{pmatrix} a_\alpha & b_\alpha \\ -b_\alpha & a_\alpha \end{pmatrix}, \quad (\alpha = I, II, III), \tag{9}$$

with $\bar{\mathcal{E}} = \mathrm{diag}(\mathcal{E}_I, \mathcal{E}_I, \mathcal{E}_{II}, \mathcal{E}_{II}, \mathcal{E}_{III}, \mathcal{E}_{III})$ and $a_\alpha \le 0$ and $\mathcal{E}_I, \mathcal{E}_{II}, \mathcal{E}_{III} \ge 0$. The RBE in the V-frame has θ-independent uncoupled parabolic operators and that will be exploited by our numerical approach.

RBE IN 2 DEGREES OF FREEDOM. FLAT RING

We now consider the case of two degrees of freedom in a flat ring with FODO cells and cavities. Moreover the case of a flat ring allows us to use a one-dimensional approach to spin which in turn allows us to average over orbit *and* spin. In our flat ring model Ω_Y has the simple form

$$\Omega_Y(\theta, Y) = -a_Y(\theta)Y\mathcal{J}, \quad \mathcal{J} = \begin{pmatrix} 0 & 1 & 0 \\ -1 & 0 & 0 \\ 0 & 0 & 0 \end{pmatrix}.$$

Here $Y \in \mathbb{R}^4$ represents the horizontal and longitudinal motions which are uncoupled from the vertical motion in the flat ring model. It is convenient to use spherical coordinates as spin variables (i.e., $\vec{S} = (\cos(\Psi)\sin(\Phi), \sin(\Psi)\sin(\Phi)), \cos(\Phi))^T$). In the Y-frame system of Langevin equations then becomes

$$Y' = (A(\theta) + \varepsilon\delta A(\theta))Y + \sqrt{\varepsilon\omega(\theta)}(0,0,0,1)^T\xi(\theta), \tag{10}$$

$$\Psi' = a_Y(\theta)Y, \tag{11}$$

$$\Phi' = 0. \tag{12}$$

Here the row vector $a_Y(\theta)$ is 2π-periodic in θ.

Following the approach outlined in previous section, we apply the method averaging and transform the current frame to a W-frame associated with an averaged problem posed in terms of a new variable W. W now incorporates both spin and phase space variable. In the W-frame the polarization density $\vec{\eta}_W$ satisfies the RBE

$$\begin{aligned} \partial_\theta\vec{\eta}_W =& -\varepsilon\sum_{j=1}^{2}\partial_{w_j}\left(\left(\mathcal{D}_I(w_1,w_2)^T\right)_j\vec{\eta}_W\right) \\ & -\varepsilon\sum_{j=3}^{4}\partial_{w_j}\left(\left(\mathcal{D}_{II}(w_3,w_4)^T\right)_j\vec{\eta}_W\right) \\ & +\frac{\varepsilon}{2}\mathcal{E}_I\left(\partial_{w_1}\partial_{w_1}+\partial_{w_2}\partial_{w_2}\right)\vec{\eta}_W \\ & +\frac{\varepsilon}{2}\mathcal{E}_{II}\left(\partial_{w_3}\partial_{w_3}+\partial_{w_4}\partial_{w_4}\right)\vec{\eta}_W \\ & -\varepsilon\sum_{j=1}^{4}\bar{\mathcal{D}}_{5j}w_j\mathcal{J}\vec{\eta}_W - \frac{\varepsilon}{2}\bar{\mathcal{E}}_{55}\vec{\eta}_W + \varepsilon\sum_{j=1}^{4}\bar{\mathcal{E}}_{j5}\mathcal{J}\vec{\eta}_W, \end{aligned} \tag{13}$$

where

$$\bar{\mathcal{D}} = \begin{pmatrix} \mathcal{D}_I & 0_{2\times2} & 0_{2\times2} \\ 0_{2\times2} & \mathcal{D}_{II} & 0_{2\times2} \\ \bar{\mathcal{D}}_{51}\ \bar{\mathcal{D}}_{52} & \bar{\mathcal{D}}_{53}\ \bar{\mathcal{D}}_{54} & 0_{1\times2} \\ 0_{1\times2} & 0_{1\times2} & 0_{1\times2} \end{pmatrix}, \tag{14}$$

$$\bar{\mathcal{E}} = \begin{pmatrix} \mathcal{E}_I & 0 & 0 & 0 & \bar{\mathcal{E}}_{15} & 0 \\ 0 & \mathcal{E}_I & 0 & 0 & \bar{\mathcal{E}}_{25} & 0 \\ 0 & 0 & \mathcal{E}_{II} & 0 & \bar{\mathcal{E}}_{35} & 0 \\ 0 & 0 & 0 & \mathcal{E}_{II} & \bar{\mathcal{E}}_{45} & 0 \\ \bar{\mathcal{E}}_{15} & \bar{\mathcal{E}}_{25} & \bar{\mathcal{E}}_{35} & \bar{\mathcal{E}}_{45} & \bar{\mathcal{E}}_{55} & 0 \\ 0 & 0 & 0 & 0 & 0 & 0 \end{pmatrix}. \tag{15}$$

Here $\mathcal{D}_I, \mathcal{D}_{II}$ are 2×2 matrices of the form (5) and $\mathcal{E}_I, \mathcal{E}_{II}$ are nonnegative. For Gaussian processes associated with (10)-(12) the polarization density $\vec{\eta}_W$ can be computed analytically.

RBE IN 1 DEGREE OF FREEDOM

We now consider the case of one degree of freedom using the model studied in [4,5]. The one degree of freedom model here is obtained from the two degrees of freedom flat ring model of the previous section by setting, in (14) and (15),

$$\begin{aligned} &0 = \mathcal{D}_{II} = \bar{\mathcal{D}}_{52} = \bar{\mathcal{D}}_{53} = \bar{\mathcal{D}}_{54} = \mathcal{E}_{II} = \bar{\mathcal{E}}_{25} = \bar{\mathcal{E}}_{35} = \bar{\mathcal{E}}_{45}\,, \\ &\mathcal{D}_I = -I_{2\times2}\,,\ \mathcal{E}_I = 1\,,\ \bar{\mathcal{E}}_{15} = -\bar{\mathcal{D}}_{51}\,,\ \bar{\mathcal{E}}_{55} = (\bar{\mathcal{E}}_{15})^2. \end{aligned} \tag{16}$$

One can justify the step from (14) and (15) to (16) as a good approximation by applying the betatron-dispersion formalism to the flat ring model [6]. With (16) the variables W_3, W_4, W_6 are uncoupled so that we are left with the following one degree of freedom system of Langevin equations for

ISBN: 978-3-95450-200-4 doi:10.18429/JACoW-ICAP2018-MOPAF04

the orbital variables W_1, W_2 and the spin variable W_5:

$$\begin{pmatrix} W_1' \\ W_2' \\ W_5' \end{pmatrix} = \varepsilon \begin{pmatrix} -1 & 0 & 0 \\ 0 & -1 & 0 \\ g & 0 & 0 \end{pmatrix} \begin{pmatrix} W_1 \\ W_2 \\ W_5 \end{pmatrix} + \sqrt{\frac{\varepsilon}{2}} \begin{pmatrix} 1 & 0 \\ 0 & 1 \\ -g & 0 \end{pmatrix} \begin{pmatrix} \xi_1 \\ \xi_2 \end{pmatrix},$$

where $g = \bar{\mathcal{D}}_{51} = -\bar{\mathcal{E}}_{15}$ and ξ_1, ξ_2 are statistically independent versions of the white noise process. Denoting the polarization density for our one degree of freedom model by $\vec{\eta}$, one can show in analogy to the previous section that it satisfies the RBE

$$\partial_\theta \vec{\eta} = \varepsilon \left(\partial_{w_1}(w_1 \vec{\eta}) + \partial_{w_2}(w_2 \vec{\eta}) \right) + \frac{\varepsilon}{4} \partial_{w_1} \partial_{w_1} \vec{\eta} + \frac{\varepsilon}{4} \partial_{w_2} \partial_{w_2} \vec{\eta} - \varepsilon g w_1 \mathcal{J} \vec{\eta} - \frac{\varepsilon}{2} g \mathcal{J} \partial_{w_1} \vec{\eta} - \frac{\varepsilon}{4} g^2 \vec{\eta}, \quad (17)$$

where $\varepsilon \approx 0.008$ and $g \approx 2.07$ for the HERA ring. We present the numerical approach to solve (17) next.

NUMERICAL APPROACH

We first transform (17) to polar coordindinates using

$$w_1 = r\cos\varphi, \quad w_2 = r\sin\varphi,$$
$$\nabla \cdot (W\eta_l) = (2 + r\partial_r)\eta_l,$$
$$\nabla \cdot \nabla \eta_l = (\partial_r^2 + r^{-1}\partial_r + r^{-2}\partial_\varphi^2)\eta_l,$$
$$\partial_{w_1}\eta_l = (\cos\varphi \frac{\partial}{\partial r} - \frac{\sin\varphi}{r}\frac{\partial}{\partial \varphi})\eta_l$$

and the RBE in 1 DOF becomes

$$\partial_t \eta_l = \frac{\varepsilon}{4}\left[\left((8 - g^2) + (4r + r^{-1})\partial_r + \partial_r^2 + r^{-2}\partial_\varphi^2 \right)\eta_l + 2g J_{lm} \left(2r\cos\varphi + \cos\varphi \partial_r - r^{-1}\sin\varphi \partial_\varphi \right)\eta_m \right], \quad l, m = 1, 2, \ l \neq m, \quad (18)$$

We pose (18) on a disk $r \leq r_{\max}$, $\varphi \in [0, 2\pi]$. The boundary conditions are periodic in φ and we take $r_{\max}$ large enough to impose homogenous Dirichlet boundary conditions at $r = r_{\max}$. Here and in the following we drop arrows and replace θ by t. We seek approximations to η on a Chebyshev grid in r and a uniform grid in φ,

$$r_i = -\cos\left(\frac{\pi i}{n_r}\right), \quad i = 0, \ldots, n_r,$$
$$\varphi_j = j\frac{2\pi}{n_\varphi}, \quad j = 1, \ldots, n_\varphi,$$

and expand it in a Fourier series in the φ direction:

$$\eta(t, r_i, \varphi_j) \approx \sum_{k=-n_{\varphi/2}+1}^{n_\varphi/2} \hat{\eta}(r_i, k, t) e^{-\imath k \varphi_j}. \quad (19)$$

For the kth Fourier mode we determine $\hat{\eta}(t, r, k)$ from

$$\partial_t \hat{\eta}_l = \frac{\varepsilon}{4}\left[\left((8 - g^2) + (4r + r^{-1})\partial_r + \partial_r^2 - r^{-2}k^2 \right)\hat{\eta}_l + g J_{lm} \left((2r + \partial_r)(\hat{\eta}_m^- + \hat{\eta}_m^+) - r^{-1}\left((k\hat{\eta}_m)^- - (k\hat{\eta}_m)^+ \right) \right) \right], \quad (20)$$

where $l, m = 1, 2$, $l \neq m$ and

$$\hat{\eta_l}^- = \hat{\eta}_l(t, r, k-1), \quad \hat{\eta_l}^+ = \hat{\eta}_l(t, r, k+1).$$

Now denote by $\hat{u}_l(t, k)$ the grid function on the r grid for a fixed mode, i.e. $\hat{u}_l(t, k) = [\hat{u}_l(t, r_0, k), \ldots, \hat{u}_l(t, r_{n_r}, k)]^T$, describes the lth component of $\hat{\eta}$. Then for each component we have

$$\frac{d\hat{u}_l(t, k)}{dt} = \frac{\varepsilon}{4}\left[F_I^k(\hat{u}_l) + J_{lm} F_E^k(\hat{u}_m) \right]. \quad (21)$$

Here F_I and F_E are linear operators representing the Fokker-Planck operator and spin terms

$$F_I(\hat{u}_l) = \left((8 - g^2)I + (4R + R^{-1})D_1 + D_2 - R^{-2}k^2 \right)\hat{u}_l,$$
$$F_E(\hat{u}_m) = \left((2R + D_1)(\hat{u}_m^+ + \hat{u}_m^-) - R^{-1}((k\hat{u}_m)^- - (k\hat{u}_m)^+ \right).$$

Here I is the $(n_r + 1) \times (n_r + 1)$ identity matrix, $R = \mathrm{diag}(r_0, \ldots, r_{n_r})$, D_1 and D_2 are spectral differentiation matrices. The entries of the differentiation matrices are found by the techniques for constructing finite difference approximations of any order of accuracy, for any order of the derivative and on general grids described by Fornberg in [7]. To be precise, the coefficients are computed using a numerically stable recursion relation derived from the Lagrange interpolant associated with the grid points (see also the subroutine `weights.f` provided in [7]). To evolve in time we use a fourth order additive N-stage Runge-Kutta scheme (ARK), see e.g. [2]. Let $\hat{u}^\nu(k) = \hat{u}(k, \nu\Delta t)$ then, for each mode, we compute

$$\hat{u}^{\nu+1} = \hat{u}^\nu + \sum_{s=1}^{N} \gamma_s \mathbf{k}_s, \quad (22)$$
$$\mathbf{k}_s = \frac{\varepsilon\Delta t}{4}\left[F_I\left(\hat{u}^\nu + \sum_{l=1}^{s} \alpha_{sl}\mathbf{k}_l \right) + F_E\left(\hat{u}^\nu + \sum_{l=1}^{s-1} \beta_{sl}\mathbf{k}_l \right) \right].$$

Thus at each step we compute $u^{\nu+1}$ given u^ν. The general N-stage ARK scheme combines N-stage diagonally implicit Runge-Kutta scheme (DIRK) with N-stage explicit Runge-Kutta scheme (ERK) of a same order of accuracy. The coefficients $\alpha_{sl}, \beta_{sl}, \gamma_s$ can be found so that the combined schemes are consistent. For higher number of DOF the algorithm stays the same.

As indicated in the introduction, the cost of the solve in (22) depends on the choice of algorithm but can always be split into an initial cost (e.g. LU-factorization in addition to the FFT) and a solve cost (e.g. back and forward substitution). Ignoring the startup cost, which can be amortized over many

ISBN: 978-3-95450-200-4 doi:10.18429/JACoW-ICAP2018-MOPAF04

time steps, the cost per time step is that of n_φ solves of size n_r for each stage, i.e. $O(n_\varphi n_r^q)$.

For 3 DOF the complexity estimate becomes

$$C = O(n_\varphi^3 n_r^{3q}).$$

Assuming that $n_r = n_\varphi = N$ we find that for $N = 50$ and $q = 1, 4/3, 2$ the cost $C = 1.5 \cdot 10^{10}, 7.8 \cdot 10^{11}$ and $2 \cdot 10^{15}$, respectively. As a single modern processing unit may be able to carry out $O(10^8 - 10^9)$ arithmetic operations per second it appears plausible that an efficient parallel implementation can result in time-per-time step on the order of one to several seconds for $q = 4/3$. Note that there are several modern solution techniques, like the Hierarchical Poincaré-Steklov operator technique by Martinsson [8] that can reach $q \approx 1$ for spectrally accurate discretizations.

NUMERICAL RESULTS

Example 1: 1 DOF model

Here the reduced Bloch Equations (17) can be solved exactly [9]. For example if

$$\eta(0, w) = \frac{2}{\pi} \begin{pmatrix} \cos(\psi_0) \\ \sin(\psi_0) \end{pmatrix} e^{-2(w_1^2 + w_2^2)}. \tag{23}$$

then

$$\eta(t, w) = \frac{2}{\pi} e^{\Sigma_2} \begin{pmatrix} \cos(\psi_0 + \Sigma_1 w_1) \\ \sin(\psi_0 + \Sigma_1 w_1) \end{pmatrix} e^{-2(w_1^2 + w_2^2)}, \tag{24}$$

$$\Sigma_1(t) = -g(1 - e^{-\varepsilon t}), \quad \Sigma_2(t) = \frac{g^2}{8}(e^{-2\varepsilon t} - 1),$$

The polarization vector of the bunch at time t is

$$P(t) = \int_{\mathbb{R}^2} \eta(t, w) dw,$$

and

$$|P(t)| = e^{-\frac{1}{8}\Sigma_1^2(t)} e^{\Sigma_2(t)}. \tag{25}$$

This example was used to verify that the polarization is computed accurately. The polarization $|P(t)|$ obtained by integrating the numerical solution, see Fig. 1. The result is very close to the exact polarization (25), within the error we expect.

In Fig. 2 the numerical solution η_1 snapshots are taken at initial time and after 25, 250 and 1500 turns (10 turns HERA ring correspond to $t = 4$) showing that the solution approaches the equilibrium

$$\eta_{eq}(w) = \frac{2}{\pi} e^{-\frac{g^2}{8}} \begin{pmatrix} \cos(\psi_0 - g w_1) \\ \sin(\psi_0 - g w_2) \end{pmatrix} e^{-2(w_1^2 + w_2^2)}. \tag{26}$$

Example 2: Spectral convergence for 1 DOF model

To confirm the spectral convergence in r and φ we evolve (18) with the initial data taken to be the exact solution (24) at $t = 0$. It has an equilibrium solution (26) making it a good test case for the numerical method. To be precise, the errors displayed in Fig. 3 are the maximum deviation from the exact solution (24) taken over all grid points and all the variables at $t = 5/\varepsilon$ which corresponds to 1500 turns. The results clearly show the spectral accuracy of the spatial discretization.

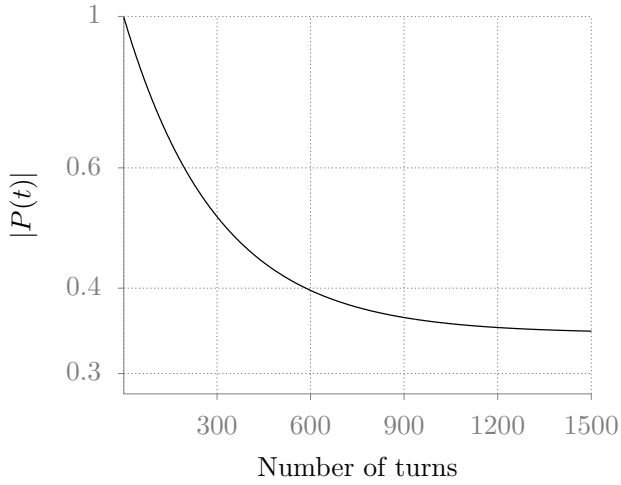

Figure 1: Polarization in 1 DOF model computed from the numerical solution.

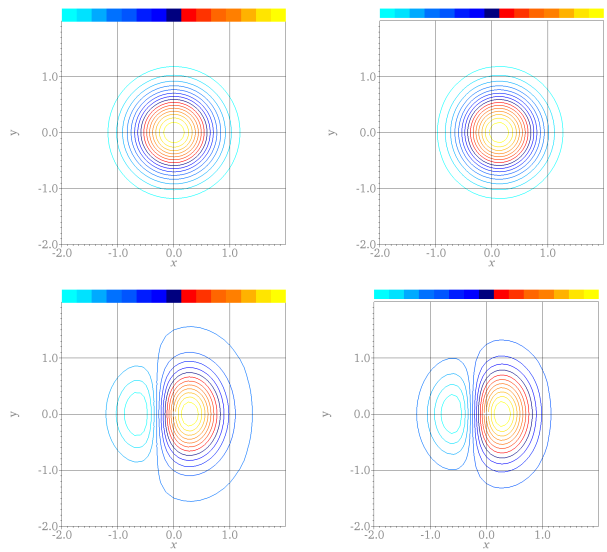

Figure 2: Solution η_1 at time $t = 0, 10, 100, 600$

DISCUSSION AND NEXT STEPS

We are preparing an extended version of this brief note for an archival journal which will complete the work on the reduced Bloch equation in 2 DOF. An important aspect will be a more detailed discussion of the algorithm. The codes will be made available in a repository. A goal is to make our work easily reproducible. Next we will incorporate the spin flip by considering the full Bloch equations and do a careful study of the depolarization and polarization effects for the simple lattice. This will include depolarization and polarization times and equilibrium. We will then study a more realistic lattice in the 2 DOF case and begin the 3 DOF work, where a parallel algorithm will surely be important/necessary.

ISBN: 978-3-95450-200-4 doi:10.18429/JACoW-ICAP2018-MOPAF04

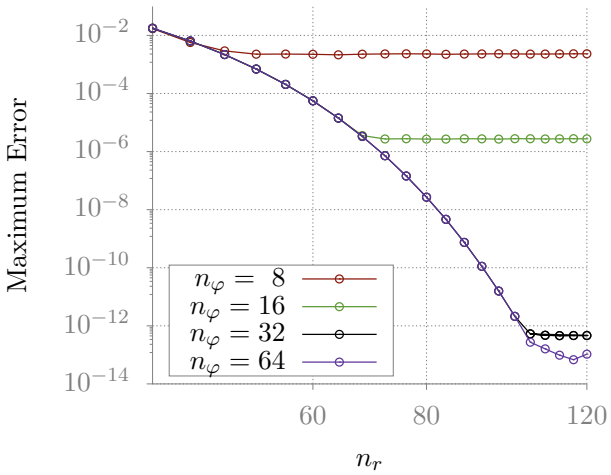

Figure 3: Convergence for the 1 DOF model.

ACKNOWLEDGEMENT

This material is based upon work supported by the U.S. Department of Energy, Office of Science, Office of High Energy Physics, under Award Number DE-SC0018008.

REFERENCES

[1] K. Heinemann, D. Appelö, D.P. Barber, O. Beznosov, J.A. Ellison, "Spin dynamics in modern electron storage rings: Computational and theoretical aspects", *Invited talk and paper, ICAP18, Key West*, Oct 19–23, 2018.

[2] C.A. Kennedy, M.H. Carpenter, "Additive Runge-Kutta schemes for convection-diffusion-reaction equations", *Appl. Numer. Math.*, vol. 44, pp. 139–181, 2003.

[3] D.P. Barber, K. Heinemann, H. Mais, G. Ripken, "A Fokker-Planck treatment of stochastic particle motion", DESY-91-146, 1991.

[4] K. Heinemann, "Some models of spin coherence and decoherence in storage rings", arXiv:physics/9709025, 1997.

[5] D.P. Barber, M. Böge, K. Heinemann, H. Mais, G. Ripken, Proc. 11th Int. Symp. High Energy Spin Physics, Bloomington, Indiana (1994).

[6] H. Mais, G. Ripken, "Spin-orbit motion in a storage ring in the presence synchrotron radiation using a dispersion formalism", DESY-86-029, 1986.

[7] B. Fornberg, "Classroom Note: Calculation of Weights in Finite Difference Formulas", *SIAM Review*, vol. 40(3), pp. 685–691, 1998.

[8] P.G. Martinsson, "A direct solver for variable coefficient elliptic PDEs discretized via a composite spectral collocation method", *J. Comput. Phys.*, vol. 242, pp. 460 – 479, 2013.

[9] K. Heinemann, unpublished notes.